buildings

MDPI

Article

Stochastic Dynamic Response and Long-Term Settlement Performance of Superstructure–Underground Tunnel–Soil Systems Subjected to Subway-Traffic Excitation

Lin Wang [1,2], Shifei Yang [2] and Hongqiang Hu [3,4,5,*]

[1] Department of Geotechnical Engineering, College of Civil Engineering, Tongji University, Shanghai 200092, China
[2] SGIDI Engineering Consulting (Group) Co., Ltd., Shanghai 200093, China
[3] Center for Balance Architecture, Zhejiang University, Hangzhou 310058, China
[4] College of Civil Engineering and Architecture, Zhejiang University, Hangzhou 310058, China
[5] The Architectural Design & Research Institute of Zhejiang University Corporation Limited, Hangzhou 310028, China
* Correspondence: huhongqiang93@163.com

Abstract: The vibration impact force from the long-term operation of a subway affects the comfort of the residents living above the superstructure and the long-term settlement deformation of the tunnel foundation. A method for evaluating the dynamic responses of superstructure–tunnel systems is important, especially because of the randomness of vibration impact force. The coupling effect of the randomness of train-vibration excitation and the nonlinearity of the geotechnical properties that are subjected to dynamic action leads to challenges in the evaluation of the performance of superstructure–underground tunnel–soil systems under train vibration. In this study, a stochastic dynamic model of subway vibration-load excitation was established; then, the time histories of samples with rich probability characteristics in the same set system were generated. According to the nonlinear dynamic finite element analysis, several nonlinear dynamic responses of the deterministic superstructure–tunnel soil-foundation system were obtained. Finally, the probabilistic performance evolution of the superstructure–tunnel soil-foundation system was obtained by integrating the first-passage and probability density evolution theories, and the long-term deformation performance of the tunnel foundation was evaluated using time-varying reliability. This study presents a novel probabilistic method and a more objective performance index for the dynamic performance assessment of superstructure–underground tunnel–soil systems that are subjected to subway-traffic excitation.

Keywords: train vibration excitation; dynamic response; time-varying reliability; long-term performance

Citation: Wang, L.; Yang, S.; Hu, H. Stochastic Dynamic Response and Long-Term Settlement Performance of Superstructure–Underground Tunnel–Soil Systems Subjected to Subway-Traffic Excitation. *Buildings* **2023**, *13*, 621. https://doi.org/10.3390/buildings13030621

Academic Editor: Giuseppina Uva

Received: 13 February 2023
Revised: 23 February 2023
Accepted: 23 February 2023
Published: 26 February 2023

1. Introduction

The long-term vibration-impact-force excitation of subway trains in service not only results in the settlement and deformation of tunnel foundations, which seriously endanger the safe operation of subways, but also affects the comfort of residents living in buildings above the tunnels. Therefore, a method for evaluating the dynamic responses of superstructure–tunnel systems that are subjected to subway vibration excitation is crucial. An earlier study found that the vibrations generated by train track interactions were transmitted to adjacent buildings through the tunnel structure and the surrounding ground, and that the vibrations produced by the walls and floors of the buildings caused secondary radiations of noise [1]. Infinite element and 2.5-dimensional finite element methods were used to study the propagation law of subway vibrations [2]. In recent years, many similar studies have been conducted to reveal the laws of ground vibrations and to establish models of ground vibrations caused by moving train loads [3–8]. Other studies have focused on the real-life monitoring of the impact of vibrations on tunnels [9,10].

Meanwhile, under the dynamic impact force of subway vibrations, the dynamic stress–strain relationship of soil exhibits three characteristics: hysteresis, nonlinearity, and strain accumulation. The combination of hysteresis, nonlinearity, and strain accumulation can reflect the entire process of the dynamic stress–strain change in soil. Rocks and soil are highly sensitive to dynamic cyclic load excitation; that is, rocks and soil have different dynamic responses under various dynamic cyclic load excitations. In consequence, the stochasticity of amplitude and spectrum characteristics from subway traffic loads must be considered under dynamic cyclic loads, such as train-vibration excitation. In addition, the vibration generated by a subway's operation is transmitted to the upper residential areas and industrial plants above the platform through the track bed, column, and platform, causing vibration of the superstructure. For residential buildings, severe vibration may cause residents to feel nervous and panic, thereby reducing the residents' quality of life [11]. For industrial plants, severe vibration may affect the healthy operation of high precision equipment that is sensitive to vibration [11].

Accordingly, combined with a stochastic model of the vibration process, the dynamic reliability evaluation of subway superstructures, with vibration acceleration as the performance index, provides a new idea for vibration-comfort evaluation, especially in evaluating buildings that do not meet appropriate comfort requirements, and effective and reasonable vibration-reduction measures can be proposed. In addition, for the long-term healthy operation of a tunnel's foundation, taking into account uneven vibration settlement, time-varying reliability is a good evaluation index to identify the time required for additional measurement and reinforcement of the tunnel's foundation. In particular, in this study, evaluations of the reliability and long-term performance of tunnel foundations are conducted, based on a stochastic dynamic analysis that considers the physical mechanism of track vibration. Random analysis does not change the physical mechanism of subway vibration, but only considers the influence of randomness on the basis of numerical analysis of the subway's vibrations.

To estimate the cumulative plastic strain of soil under cyclic loading, several calculation models have been proposed [12]. Currently, a modified model is commonly used. The modified model was developed on the basis of numerous studies [13–15]. Under train-vibration excitation, the dynamic response of a soil system with a superstructure–tunnel foundation shows strong nonlinearity. The amplitude and spectrum characteristics of the system's dynamic response vary with changing time histories of train vibrations and impact force; that is, the system is highly sensitive to the time histories of train vibrations and impact force. For the modeling and dynamic response analysis of moving dynamic excitation on a multi-layer stratum, some scholars considered the dynamic nonlinear characteristics of the stratum or foundation and studied the nonlinear dynamic response of a porous medium composite stratum or foundation by means of a dynamic nonlinear time-history analysis, which provided a reference and a good foundation for considering the dynamic response of a rock soil stratum or foundation under a moving load [16–18]. Additionally, due to the influence of railway track irregularities, train-vibration impact force shows considerable randomness; for this force, the effect of the random excitation load is the dominant factor. Therefore, the randomness of the train-vibration impact force must be considered in the nonlinear dynamic response analysis of soil systems with superstructure–tunnel foundations that are subjected to train-vibration excitation. Some scholars have studied the dynamic responses of soil systems with superstructure–tunnel foundations through experiments, numerical analyses, and random probability analyses [19–25]. However, the combination of the nonlinearity of a system under dynamic action and the randomness of train vibration excitation increases the difficulty in carrying out a stochastic nonlinear dynamic response analysis of soil systems with superstructure–tunnel foundations.

In consequence, this study investigated the time-varying performance of soil systems with superstructure–tunnel foundations from the perspective of the probability density function (PDF) evolution of system dynamic performance. This study established a stochas-

tic dynamic model of the subway traffic load based on describing the uncertainty of subway traffic-load excitation. Then, according to nonlinear dynamic finite element calculations, the dynamic response of a superstructure–tunnel system that was subjected to train-dynamic-impact excitation was obtained. Subsequently, according to the building-vibration-acceleration criterion, the vibration comfort of the residents living in the buildings located above the tunnel was evaluated on the basis of dynamic reliability. Furthermore, using the dynamic cyclic settlement model, the long-term settlement of rocks and soil in the subway tunnel under cyclic dynamic loads was also predicted. Moreover, by utilizing the first-passage probability method based on probability density evolution theory (PDET), the time-varying dynamic reliability of tunnel rocks and soil was obtained under cyclic dynamic loads. This time-varying reliability can provide a reference for long-term performance evaluations of subway tunnels.

2. Stochastic Simulation of the Subway-Train Impact-Force Load

The subway vibration load is a type of the cyclic load produced by running subway trains. The impact of the trains on tracks is the main cause of the dynamic response and deformation of the superstructure, the tunnel structure, and the foundation soil. From the analysis of train-vibration excitation, the train-excitation load mainly includes moving constant and stochastic excitation loads. The constant load is the train axle load, and the stochastic excitation load is the dynamic wheel-rail force resulting from the random irregularity of the tracks. The influence of the random excitation load is the main factor [26,27]. Therefore, the characterization and modeling of the train-random-excitation load must be based on train-track coupling dynamic analyses under the influence of the random irregularity of the tracks. For the long-term settlement performance prediction of subway tunnels, the establishment of a dynamic cyclic load model of the subway is a prerequisite, especially in characterizing the stochastic uncertainty of a subway dynamic load in strength and spectrum characteristics. Additionally, these factors directly affect the accuracy and rationality of numerical calculations and evaluation results. Many scholars have modeled train random excitation and have achieved considerable progress. Three methods are commonly used to determine the subway train load: analytical simulations, theoretical models, and field tests.

Analytical simulation is a suitable approach to express the stochastic excitation load of a train. Because the field test and the numerical calculation model are restricted by some conditions, the empirical-formula-based simulation of train-vibration excitation is widely applied. In railway-environment vibration, the deformation of the foundation and the buildings is considerably small, and the vehicle-track subgrade-foundation model can be considered as a linear system; thus, the analytical simulation method presents obvious advantages. The analytical simulation not only reflects ride irregularity, additional dynamic loads, and rail-surface-waveform losses, but also considers the movement of the train wheelset force on the line, the superposition combination, and the scattered transmission of the rail and the pad.

To describe dynamic wheel-rail force resulting from random track irregularity in the stochastic excitation load, this study established a stochastic excitation model to understand the subway impact force on the basis of spectral representation. For the subsequent stochastic dynamic response analyses and the long-term performance evaluation of the superstructure–subway tunnel soil system, the stochastic function concept was introduced to reduce the sample size in deterministic nonlinear dynamic analyses and, ultimately, to minimize the calculations in the nonlinear stochastic dynamic analyses.

2.1. Power Spectrum of the Train-Stochastic-Excitation Load by the Pseudo-Excitation Method (PEM)

The track irregularity power spectrum is the most effective tool to describe the track irregularity of an entire tunnel. Various global national codes and relevant literature have proposed the track power spectrum to describe track irregularity [28] and long-term vibrational behavior [29]. However, the power spectrum of track irregularity cannot be

directly discretized to obtain the impact force of subway vibrations, which cannot be directly applied to the establishment of the random excitation model for trains and the generation of sample time histories. Therefore, the track irregularity power spectrum must be transformed into the train stochastic excitation power spectrum.

The time histories of track irregularity samples are generated through the power spectral density (PSD) of track irregularity. Then, the time domain response of the random excitation load is calculated by using numerical integration or analytical methods. The power spectrum of the stochastic excitation load of the train can be estimated using the Fourier transform of time domain response, which may lead to a large errors of analysis because of time-domain sample generation or PSD estimation. This study obtained the power spectrum of the train-random-excitation load directly from the power spectrum of track irregularity by employing PEM [29]. PEM presents the advantage that the power spectrum (the train-random-excitation load) output can be obtained directly from the power spectrum (track irregularity) input.

In the model, track irregularity is assumed to be harmonic, and the moving vehicle is idealized as a multi-rigid body system connected via springs and dampers; the ballasted track and subgrade are considered elastic multi-layer beams; and the embankment foundation is considered a semi-infinite space. Furthermore, the dynamic wheel-rail-force equation can be written as follows [30]:

$$(C_W + C_R + C_\Delta)\{F(\omega)\} = \{\Delta y(\omega)\}, \tag{1}$$

where C_W and C_R are the flexibility matrices of the vehicle at the wheel set and the ballast track subgrade foundation system at the wheel-rail contact point, respectively; C_Δ is the linear Hertz contact flexibility coefficient matrix of the wheel rail; $\Delta y(\Omega)$ is the track surface harmonic irregularity at the wheel-rail contact point; and $F(\omega)$ is the dynamic wheel-rail force amplitude.

If the time-history function $\Delta y(t)$ of track irregularity random excitation is used to represent the stationary impact force on the dynamic system, then according to the PEM, the corresponding pseudo-excitation can be expressed as follows:

$$\Delta\widetilde{y}(t) = \sqrt{S_v(\omega)}e^{i\omega t}, \tag{2}$$

where $S_v(\omega)$ is the self-spectrum density of $\Delta y(t)$. Then, the pseudo-excitation corresponding to $\Delta y(t)$ becomes:

$$\begin{array}{ll} \Delta y(t) & = \exp(-i\omega t)\sqrt{S_v(\omega)}e^{i\omega t} \\ & = \Delta\widetilde{y}(\omega)e^{i\omega t} \end{array}, \tag{3}$$

where $\Delta\widetilde{y}(\omega)$ is the amplitude of the pseudo-excitation of track harmonic irregularity.

Substituting the pseudo-excitation $\Delta\widetilde{y}(\omega)$ of the track harmonic irregularity amplitude presented in Equation (3) in Equation (1) to replace $\Delta y(\omega)$, we obtain:

$$(C_W + C_R + C_\Delta)\left\{\widetilde{F}(\omega)\right\} = \{\Delta\widetilde{y}(\omega)\}. \tag{4}$$

where $\widetilde{F}(\omega)$ is the pseudo-dynamic-wheel-rail-force amplitude corresponding to pseudo-excitation, $\Delta\widetilde{y}(\omega)$.

The pseudo-dynamic-wheel-rail-force amplitude resulting from pseudo-track irregularity can be calculated using Equation (4). Then, according to PEM, the actual PSD of the dynamic wheel-rail impact force can be obtained as follow:

$$S_{pp}(\omega) = \left\{\widetilde{F}(\omega)\right\}^* \{F(\omega)\}^T. \tag{5}$$

where $\left\{\widetilde{F}(\omega)\right\}^*$ and $\{F(\omega)\}^T$ are the conjugate and transpose of $\{F(\omega)\}$, respectively.

Because the power spectrum of track irregularity is usually a one-sided power spectrum $S_v(\alpha)$ expressed through spatial–circular frequency and $S_v(\omega)$ is a temporal power spectrum, the power spectrum of track irregularity must be converted into the one-sided power spectrum expressed through temporal–circular frequency. If the time circle frequency $\omega = \alpha D$ and α is the space circle frequency, the time power spectrum $S_v(\omega)$ is expressed as follows:

$$S_v(\omega) = \frac{S_v(\alpha)}{D}. \tag{6}$$

By substituting Equation (6) into Equation (5) and applying the aforementioned PEM method, the one-sided PSD $S_{pp}(\omega)$ of train dynamic excitation resulting from track irregularity can be obtained.

The accurate PSD of the train-random-excitation load is obtained directly through the PSD of PEM-based track irregularity. PEM reduces the analysis error in the time-domain sample inversion of the track spectrum and power spectral estimation through the time-domain response in the conventional method and considerably minimizes calculation work. In this study, the vehicle-track vertical transverse coupling model [31] is used to describe and express the randomness of vibration excitation, and the power spectral density (PSD) function for the train speed, $V_{\text{subway}} = 44.44$ m/s, is selected to determine the discrete time history of the subway-vibration-excitation samples.

2.2. Generation of Stochastic Excitation Samples from Subway Vibration

According to the measured load records, subway-vibration excitation can be considered a zero mean stationary random process, $F(t)$. Assume that the single-side power spectrum of $F(t)$ is $U_F(\omega)$. Then, the classical spectral representation of the stationary random process $F(t)$ based on orthogonal random variables can be expressed as follows:

$$F(t) = \sum_{k=1}^{N} \sqrt{U_F(\omega_k)\Delta\omega}[u_k \cos(\omega_k t) + v_k \sin(\omega_k t)], \tag{7}$$

where $\Delta\omega$ is the discrete frequency step; N is the number of frequency truncation terms; ω_1 and ω_N are the upper and lower cut-off frequencies, respectively; and $\{u_k, v_k\}$ is the set of standard orthogonal random variables. The relationship between these physical quantities is determined as follows:

$$\begin{cases} \Delta\omega = \frac{\omega_N - \omega_1}{N-1} \\ \omega_k = \omega_1 + (k-1)\Delta\omega \end{cases}. \tag{8}$$

In Equation (7), let u_k and v_k be

$$\begin{cases} u_k = \sqrt{2}\cos\varphi_k \\ v_k = \sqrt{2}\sin\varphi_k \end{cases}, \tag{9}$$

where $\varphi_k (k = 1, 2, \cdots, N)$ is the group of independent random variables that obey the uniform distribution on $[0, 2\pi]$. u_k and v_k are orthogonal random variables.

The classical spectral representation can be obtained by substituting Equation (9) into Equation (7), as follows:

$$F(t) = \sqrt{2}\sum_{k=1}^{N} \sqrt{U_F(\omega_k)\Delta\omega}\cos(\omega_k t - \varphi_k). \tag{10}$$

Equation (10) is the spectral representation based on the random phase angle. According to the aforementioned transformation, Equation (10) is a special case of Equation (7).

Equation (9) is a constraint on orthogonal random variables. Thus, the number of random variables is decreased from $2N$ in Equation (7) to N in Equation (10). The number of random variables in the simulation formula of spectral representation may considerably decrease if strict constraints are imposed on the standard orthogonal random variables.

Therefore, according to the random function concept, $\{u_q, v_q\}(q = 1, 2, \cdots, N)$ can be expressed as the orthogonal function of the basic random variable Θ:

$$\begin{cases} u_q = \sqrt{2}\cos\left(q\Theta + \frac{\pi}{4}\right) \\ v_q = \sqrt{2}\sin\left(q\Theta + \frac{\pi}{4}\right) \end{cases}, \tag{11}$$

in Equation (2), where Θ is the basic random variable uniformly distributed in the interval $(-\pi,\ \pi)$.

Using the discrete method of the aforementioned random model, the time-history samples of the stationary random process of the subway vibration impact force can be obtained (Figure 1a). To verify the rationality and effectiveness of the generated impact time-history sample set, the average power spectrum of the sample set must be compared with the target power spectrum. In Figure 1b, the red dotted line represents the collective power spectrum of the impact time-history samples, and the blue solid line shows the target power spectrum. In this paper, the impact time-history samples were obtained by discretizing the target power spectrum; that is, according to the time-history sample set, the discrete target power spectrum used to obtain the impact time-history samples and the average power spectrum were a pair of inverse processes. To ensure that the target power and the average power spectra of the impact force time-history sample set fit well, the number of the impact force time-history samples was adjusted until the fitting error of these two was controlled within the range that satisfied engineering requirements. The fitting error shown in Figure 1b was 0.98%, and the number of samples corresponding to the impact force time history was 1000.

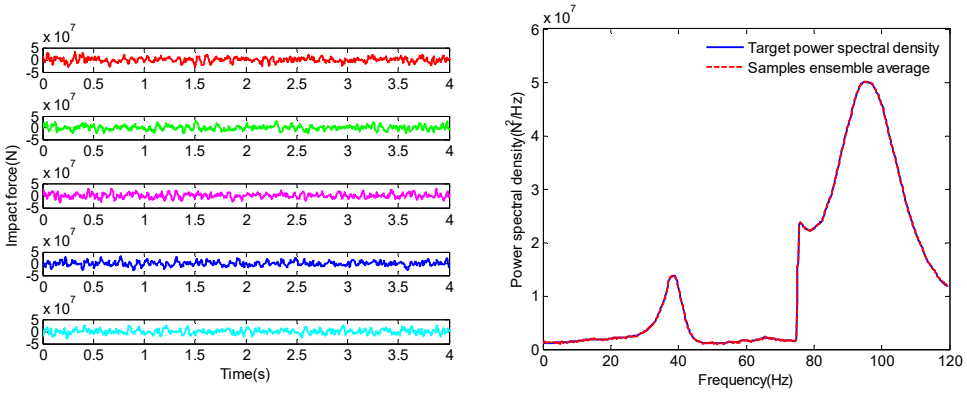

(**a**) (**b**)

Figure 1. (**a**) Typical time-history sample of wheel-rail impact force. (**b**) Comparison of ensemble average of the impact samples and target PSD.

3. Stochastic Dynamic Response of the Superstructure and Soft Soil under Subway-Traffic Excitation

To determine the stochastic dynamic reliability performance of the superstructure and the tunnel foundation subjected to subway-vibration excitation, this study introduced nonlinear-stochastic-dynamics-based PDET [32,33]. The spectral representation and random function of railway stochastic excitation for probabilistic information, such as PDF, are consistent with PDET. The combination of the two methods can provide an efficient and accurate technique for the stochastic dynamic response analysis of superstructure–tunnel soil coupling nonlinear systems. The combined technique can also be used for the fine analysis of the dynamic response of the superstructure and the tunnel railway load and to provide a reference for long-term performance evaluation.

3.1. Numerical Analysis Model of a Superstructure–Underground-Tunnel System under Subway-Traffic Excitation

Because the stochastic dynamic response analysis of the superstructure–tunnel system is based on its effective deterministic dynamic response analysis, its deterministic dynamic response is important for obtaining its PDF and other stochastic information. The dynamic response of the superstructure–tunnel system subjected to the impact force of subway vibration can be obtained by conducting the finite-element dynamic analysis in Midas GTS NX (New eXperience of Geo-Technical analysis System) [34]. Figure 2 illustrates the finite-element model of the superstructure–tunnel system.

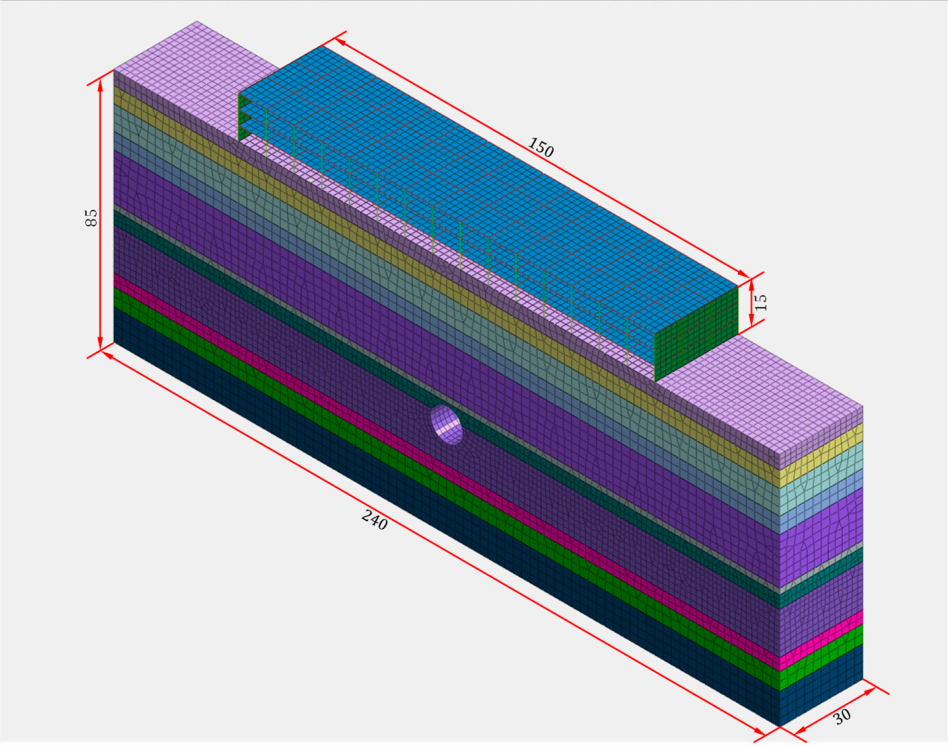

Figure 2. Finite-element model of the superstructure-underground-tunnel system (Unit: m).

In the finite-element model, the soil can be modeled using the solid element, and the beam, column, and floor are simulated through beam and plate elements. In the finite-element model of the superstructure–tunnel system, the sum of the number of solid, beam, and plate elements is 12541. The computation work of the dynamic time-history analysis of such a model is not applicable and it is unrealistic for Monte–Carlo stochastic simulation, which is an important starting point of this study. Additionally, in the finite-element model of the superstructure–tunnel system, the linear elastic constitutive model is adopted for the superstructure. Considering the nonlinearity of the soil, the hardening-soil model proposed by Schanz T is adopted [35]. According to the top-to-bottom order of soil layers, the specific constitutive parameters are presented in Table 1. In this paper, E_1 is the secant stiffness of the triaxial test of the rocks and soil, E_2 is the unloading elastic modulus, n_0 is the porosity, φ is the internal-friction-angle of the rocks and soil, ψ is the shear-expansion angle, and c is the cohesion of the rocks and soil. v, ξ, and γ are Poisson's ratio, the damping ratio, and the unit weight of the rocks and soil, respectively. Moreover, beams, columns, and plates are elastic materials, with elastic modulus E_0 of 35 MPa, Poisson's ratio v of 0.3, and unit weight γ of 25 kN/m^3.

Table 1. Constitutive parameters used in the finite-element analysis in Midas/GTS.

Parameters / Soil Layers	E_1(MPa)	E_2(MPa)	n_0	φ(°)	ψ(°)	c(kPa)	v	ξ	γ(kN/m^3)
1	3	15	0.49	15	0	15	0.42	5%	18
2-3	6	24	0.46	30.5	0.5	7	0.42	5%	18
4	1.5	7.5	0.58	12	0	14	0.46	5%	16.9
5-1	4	20	0.53	14	0	17	0.42	5%	17.6
5-3-1	9	45	0.5	20.5	0	18	0.38	5%	18
5-4	16	80	0.41	17	0	45	0.41	5%	19.6
7	38	108	0.41	34	4	2	0.37	5%	19.3
8-1	12	60	0.5	18	0	21	0.40	5%	18
8-2	17	85	0.38	20	0	25	0.38	5%	18.4
9-1	61	183	0.4	36	6	0	0.33	5%	19.6
9-2-1	85	260	045	37	7	0	0.32	5%	20.1

Here, it needs to be further explained that in this study, the deterministic dynamic response analysis of the superstructure–tunnel system adopts the nonlinear dynamic time-history analysis in time domain, rather than the frequency domain analysis method. This is because this study focuses more on geotechnical engineering or soil-dynamics problems. Under the dynamic action of subway-vibration excitation, soil as a kind of geomaterial medium shows an almost nonlinear mechanical behavior, so it is obviously reasonable to apply dynamic time-history analysis. For the vibration excitation of a subway track, because the material of the train and the track is steel and has large stiffness, it is obviously a better choice to model the vibration excitation based on the frequency-domain-analysis method. In this study, the essence of the PEM method used for simulation of subway-vibration excitation is also a frequency domain method.

3.2. Stochastic Dynamic Response of the Superstructure–Tunnel System

In general, the description of the objective physical world or objective events can be divided into sample orbit (deterministic level), ensemble average (e.g., mean and variance), and transient PDF. Transient PDF is the most essential description of the objective physical world, especially for superstructure–tunnel soil dynamic systems. To obtain the transient PDF of a system, this study introduced PDET to acquire the evolution history of the PDFs of the time-related physical quantities. Then, according to the first-passage theory, the time-dependent reliability of these physical quantities was obtained and the probabilistic time-varying performance of the system was evaluated. To investigate the comfort levels of the subway-vibration impact force for residents living in the buildings above the tunnel, the dynamic acceleration of the buildings located above the tunnel was selected as the related physical quantity.

For the aforementioned superstructure–tunnel dynamic system, the dynamic differential equation under subway-vibration excitation can be expressed as follows:

$$[M]\left\{\ddot{X}\right\} + [C]\left\{\dot{X}\right\} + \left\{f\left(\dot{X}, X\right)\right\} = F(t), \tag{12}$$

where M and K are the mass and stiffness matrices, respectively. X is the dynamic response time history of the system under subway-vibration excitation. $f\left(\dot{X}, X\right)$ is the nonlinear dynamic recovery force model of the system. When $f(X) = KX$, Equation (12) becomes a linear system. $F(t)$ is the time history of subway-vibration excitation.

If the randomness of the subway-vibration excitation load is considered, Equation (12) can be rewritten as follows:

$$[M]\left\{\ddot{X}\right\} + [C]\left\{\dot{X}\right\} + \left\{f\left(\dot{X}, X\right)\right\} = F(\boldsymbol{\Theta}, t). \tag{13}$$

where $\boldsymbol{\Theta} = \left\{\theta_1, \theta_2, \cdots, \theta_q\right\}$ is the random vector reflecting the randomness of subway-vibration load excitation.

Equation (13) presents a well-posed dynamical system, and its solution exists, is unique, and depends on the external excitation and initial conditions of the system. When the initial condition is deterministic and the external excitation has randomness $\boldsymbol{\Theta}$, its solution must depend on external excitation, $F(\boldsymbol{\Theta}, t)$. For the concerned physical quantities, such as structural displacement or tunnel-foundation settlement $S(t)$ of the superstructure–tunnel soil system:

$$\boldsymbol{S}(t) = \boldsymbol{G}(\boldsymbol{\Theta}, t). \tag{14}$$

The component form of $\boldsymbol{S}(t)$ can be expressed as follows:

$$S_q(t) = G_q(\boldsymbol{\Theta}, t),\ q = 1, 2, \cdots, n_d. \tag{15}$$

Similarly, the velocity of $\dot{\boldsymbol{S}}(t)$ is a function of $\boldsymbol{\Theta}$, and it can be denoted as follows:

$$\dot{\boldsymbol{S}}(t) = \boldsymbol{L}(\boldsymbol{\Theta}, t). \tag{16}$$

Then, $L(\boldsymbol{\Theta}, t) = \partial \boldsymbol{G}(\boldsymbol{\Theta}, t)/\partial t$.

In general, the physical quantities related to practical engineering can be determined using the structure state (displacement and velocity). For example, the strain of a structure can be estimated using the partial derivative of the displacement. Thus, if $\boldsymbol{Y} = (S_1, S_2, \cdots, S_m)^T$ is the physical quantity to be considered, then

$$\dot{\boldsymbol{Y}}(t) = \psi\left[\boldsymbol{S}(t), \dot{\boldsymbol{S}}(t)\right], \tag{17}$$

where $\psi[\cdot]$ is the transformation operator from the state vector to the physical quantity under investigation. For the linear structure system, $\psi[\cdot]$ is a linear operator; for the nonlinear structure system, $\psi[\cdot]$ is a nonlinear operator. Substituting Equations (14) and (16) into Equation (17), we obtain

$$\dot{\boldsymbol{Y}}(t) = \psi[\boldsymbol{G}(\boldsymbol{\Theta}, t), \boldsymbol{L}(\boldsymbol{\Theta}, t)] = \boldsymbol{l}(\boldsymbol{\Theta}, t). \tag{18}$$

Because of the randomness of $\boldsymbol{\eta}$, it is a stochastic equation of the state, and its component form can be expressed as follows:

$$\dot{Y}_q(t) = l_q(\boldsymbol{\Theta}, t); q = 1, 2, \cdots, m. \tag{19}$$

The equation of the state (Equation (10)) is a decoupled expression; that is, the concerned physical quantities are observed separately rather than together. For the equation of the state, obtaining the evolution process is important, and whether the explicit expression of a can be obtained is irrelevant.

In the stochastic dynamic system (Equation (18)), the augmented system $(\boldsymbol{Y}(\boldsymbol{t}), \boldsymbol{\Theta})$ is conservative stochastic; that is, all random factors are included. The joint PDF of $(\boldsymbol{Y}(\boldsymbol{t}), \boldsymbol{\Theta})$ is denoted as $p_{\boldsymbol{Y\Theta}}(\boldsymbol{y}, \boldsymbol{\theta}, t)$. For the concerned random event $\{(\boldsymbol{Y}(t), \boldsymbol{\Theta}) \in \Omega_t \times \Omega_{\boldsymbol{\theta}}\}$, $\Omega_{\boldsymbol{\theta}}$ is any region in the distribution space of $\boldsymbol{\theta}$, and Ω_t is the related region in the distribution space of $\boldsymbol{Y}$ at time t. According to the conservation principle of random events,

$$\Pr\{(\boldsymbol{Y}(t), \boldsymbol{\Theta}) \in \Omega_t \times \Omega_{\boldsymbol{\theta}}\} = \Pr\{(\boldsymbol{Y}(t + \mathrm{d}t), \boldsymbol{\Theta}) \in \Omega_{t+\mathrm{d}t} \times \Omega_{\boldsymbol{\theta}}\}, \tag{20}$$

where $\Pr\{\cdot\}$ is the probability measure of a random event. The integral form of Equation (20) is expressed as follows:

$$\int_{\Omega_t \times \Omega_{\boldsymbol{\theta}}} p_{\boldsymbol{Y\Theta}}(y, \boldsymbol{\theta}, t)\mathrm{d}\boldsymbol{y}\mathrm{d}\boldsymbol{\theta} = \int_{\Omega_{t+\mathrm{d}t} \times \Omega_{\boldsymbol{\theta}}} p_{\boldsymbol{Y\Theta}}(y, \boldsymbol{\theta}, t + \mathrm{d}t)\mathrm{d}\boldsymbol{y}\mathrm{d}\boldsymbol{\theta}. \tag{21}$$

At time $t + \mathrm{d}t$ after an infinitesimal element of time $\mathrm{d}t$, $\Omega_{t+\mathrm{d}t}$ is the result of the superposition of Ω_t and its boundary motion:

$$\begin{array}{ll} \Omega_{t+\mathrm{d}t} & = \Omega_t + \int_{\partial\Omega_t} (\boldsymbol{v}_{\boldsymbol{y}}\mathrm{d}t) \cdot \boldsymbol{n}\mathrm{d}s \\ & = \Omega_t + \int_{\partial\Omega_t} (\boldsymbol{l}(\boldsymbol{\theta}, t)\mathrm{d}t) \cdot \boldsymbol{n}\mathrm{d}s \end{array}. \tag{22}$$

The velocity $\boldsymbol{v}_{\boldsymbol{y}} = \boldsymbol{l}(\boldsymbol{\theta}, t)$ determined using the state physics evolution equation (Equation (9)) shows that boundary motion and the probability density evolution are the results of system-state evolution. Therefore, by substituting Equation (22) into Equation (21) and eliminating the same term, we acquire

$$\int_{\Omega_t \times \Omega_{\boldsymbol{\theta}}} \left(\frac{\partial p_{\boldsymbol{Y\Theta}}(\boldsymbol{y}, \boldsymbol{\theta}, t)}{\partial t} \mathrm{d}t \right) \mathrm{d}\boldsymbol{y}\mathrm{d}\boldsymbol{\theta} = -\int_{\Omega_t \times \Omega_{\boldsymbol{\theta}}} \sum_{k=1}^{m} \frac{\partial [p_{\boldsymbol{Y\Theta}}(\boldsymbol{y}, \boldsymbol{\theta}, t) l_k(\boldsymbol{\theta}, t)\mathrm{d}t]}{\partial y_k} \mathrm{d}\boldsymbol{y}\mathrm{d}\boldsymbol{\theta}. \tag{23}$$

By taking the arbitrariness of $\Omega_t \times \Omega_{\boldsymbol{\theta}}$ and eliminating $\mathrm{d}t$ from both the sides of the equation, the density evolution equation can be obtained, as follows:

$$\frac{\partial p_{\boldsymbol{Y\Theta}}(\boldsymbol{y}, \boldsymbol{\theta}, t)}{\partial t} + \sum_{k=1}^{m} \dot{Y}_k(\boldsymbol{\theta}, t) \frac{\partial p_{\boldsymbol{Y\Theta}}(\boldsymbol{y}, \boldsymbol{\theta}, t)}{\partial y_k} = 0. \tag{24}$$

In this manner, by solving Equation (24), the PDF $p_{\boldsymbol{Y}}(y, t)$ of $\boldsymbol{Y}(t)$ can be obtained.

$$p_{\boldsymbol{Y}}(y, t) = \int p_{\boldsymbol{Y\Theta}}(\boldsymbol{y}, \boldsymbol{\theta}, t)\mathrm{d}\boldsymbol{\theta}. \tag{25}$$

To evaluate the dynamic evolution performance of the superstructure–tunnel soil system under subway-vibration excitation, several story drift angles $\{Y(\boldsymbol{\theta}_q, t)\}(q = 1, 2, \cdots, N_{sel})$ of the superstructure are selected as the performance index and substituted into the probability density evolution equation (PDEE) (Equation (24)); the PDEE of $\boldsymbol{Y}(\boldsymbol{\theta}, t)$ can be expressed as follows [32,33,36,37]:

$$\frac{\partial p_{\boldsymbol{Y\Theta}}(\boldsymbol{y}, \boldsymbol{\theta}, t)}{\partial t} + \dot{\boldsymbol{Y}}(\boldsymbol{\theta}, t) \frac{\partial p_{\boldsymbol{Y\Theta}}(\boldsymbol{y}, \boldsymbol{\theta}, t)}{\partial y} = 0. \tag{26}$$

Abundant probability information of interlayer displacement, such as the PDF and dynamic reliability, can be obtained by solving Equation (26). Unfortunately, it is difficult to obtain the closed-form analytical solution of the probability density evolution equation, which can be solved by numerical methods such as the finite-element method and the finite-difference method. The specific numerical solution process is shown in Figure 3, and the specific solution steps are as follows [32,38]:

(1) First, discrete representative samples points $\Theta_q(q = 1, 2, \cdots, N_{sel})$ are obtained in multidimensional random variable space Ω_Θ;

(2) Under the condition of $\Theta = \theta_q$, the nonlinear differential equations of the dynamic system, Equation (13), are respectively analyzed by deterministic dynamic analysis, based on the finite-element nonlinear dynamic time-history method, to obtain the required speed information $\dot{Y}(\theta_q, t)$;

(3) Substitute $\dot{Y}(\theta_q, t)$ as the velocity quantity into Equation (26), determine the numerical solution according to the finite difference, then perform numerical integration on Equation (25) to finally obtain the numerical solution of $p_{\boldsymbol{Y}}(y, t)$.

To evaluate and analyze the dynamic vibration comfort levels of the superstructure combined with the subway-track impact force time-history samples presented in Section 2.2, several acceleration time-history responses with assigned probabilities were obtained, using the dynamic time-history analysis by employing the finite element analysis described in Section 3.1. To reduce the amount of calculation effectively, in this calculation, the number of vibration and impact-force samples selected was $n_{\mathrm{sel}} = 254$; however, the fitting error between the set average PSD of these vibration and impact force samples and the target

PSD is controlled within 5%; that is, $\varepsilon = 4.87\%$. The velocity of the aforementioned acceleration-time-history responses and their assigned probabilities are substituted into Equation (26) as initial conditions, and the corresponding stochastic information of the vibration-acceleration response of the superstructure is obtained numerically using the finite difference method described in Equation (26).

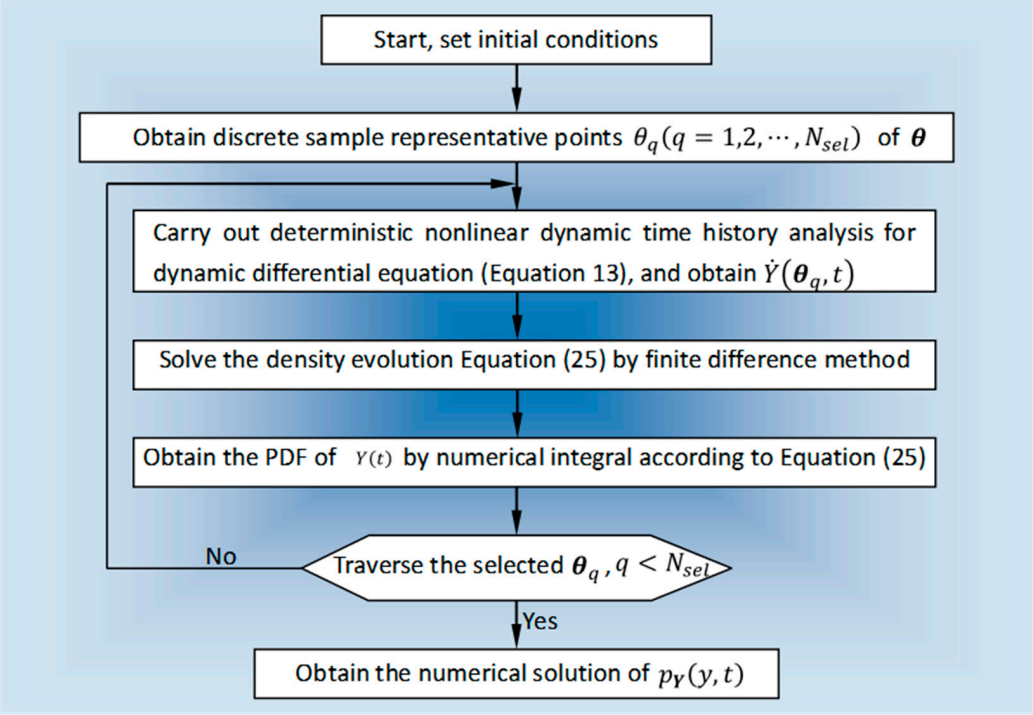

Figure 3. Numerical solution flow of PDF for the vibration-acceleration response of superstructure.

According to the probability density evolution analysis, the stochastic probability information of the dynamic response (mainly acceleration) of the superstructure subjected to the impact force of subway vibration can be obtained. Figure 4 shows the ensemble-average-evolution characteristics of the dynamic acceleration of the concerned physical quantity with vibration comfort levels. At the beginning of vibration, the acceleration response of the superstructure varies; that is, the randomness of the vibration impact force of the subway is transmitted to the acceleration response of the superstructure (Figure 4). In addition, the evolution of the mean and standard deviation with time shows that the standard deviation is at least one order higher than the mean for the magnitude order (Figure 4), which indicates that the vibration-acceleration response of the superstructure varies. The ensemble average characteristics of the vibration acceleration of the superstructure are obtained. However, the PDF is the most authentic representation of objective physical events. Therefore, for stochastic dynamic analyses, obtaining the PDF of the response is the ultimate research goal. This study also obtained the PDF of the vibration-acceleration response of the superstructure, which is an important parameter for evaluating the vibration comfort levels of the superstructure from the perspective of dynamic reliability. Figure 5 presents the PDF of the vibration-acceleration response of the superstructure at different time intervals.

Furthermore, to investigate the vibration comfort levels of the superstructure under the vibration impact of the subway, the vibration dynamic reliability of the superstructure must be analyzed. Under the action of different vibration-excitation time histories of the subway, the superstructure has a complex failure mode. According to the equivalent extreme-value principle, the structural reliability analysis under the general complex-failure criteria is transformed into the probability calculation of equivalent extreme-value events.

In this study, the reliability of the vibration-comfort evaluation of the superstructure can be expressed as

$$\mathrm{Pr} = P\left\{\cup_{q=1}^{N_{sel}}\left(g_q(\boldsymbol{\Theta}, t) > 0\right)\right\}, \tag{27}$$

where $g_1(\boldsymbol{\Theta})$, $g_2(\boldsymbol{\Theta})$, $\cdots$, $g_{N_{sel}}(\boldsymbol{\Theta})$ is the limit state function of the superstructure under each vibration excitation, so the equivalent extreme value can be constructed:

$$Z_{\max,\,T} = \max_{1 \le q \le N_{sel}} Y_q(\boldsymbol{\Theta}, t). \tag{28}$$

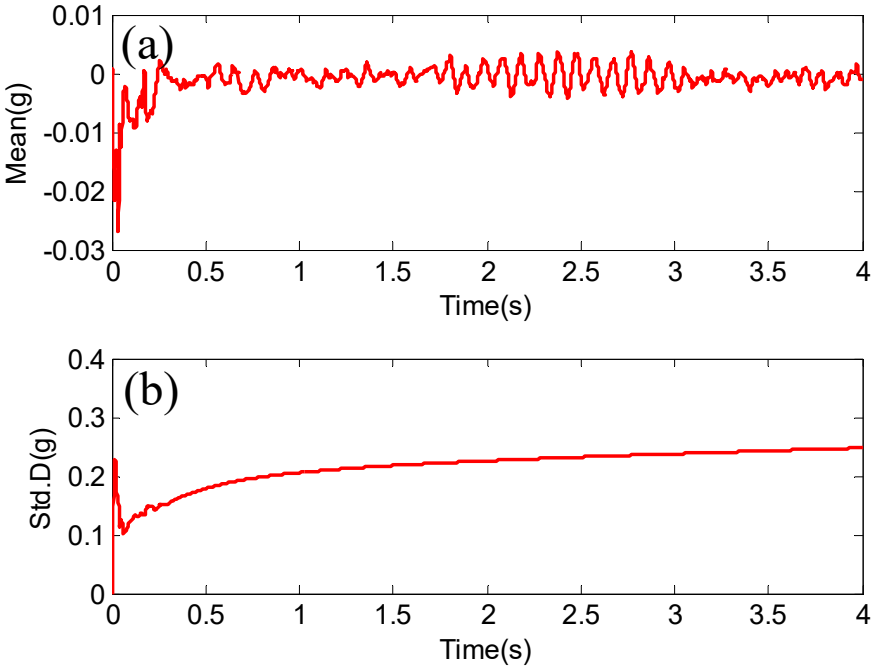

Figure 4. Ensemble average characteristics of the vibration acceleration of the superstructure of the tunnel: (**a**) mean; (**b**) standard deviation.

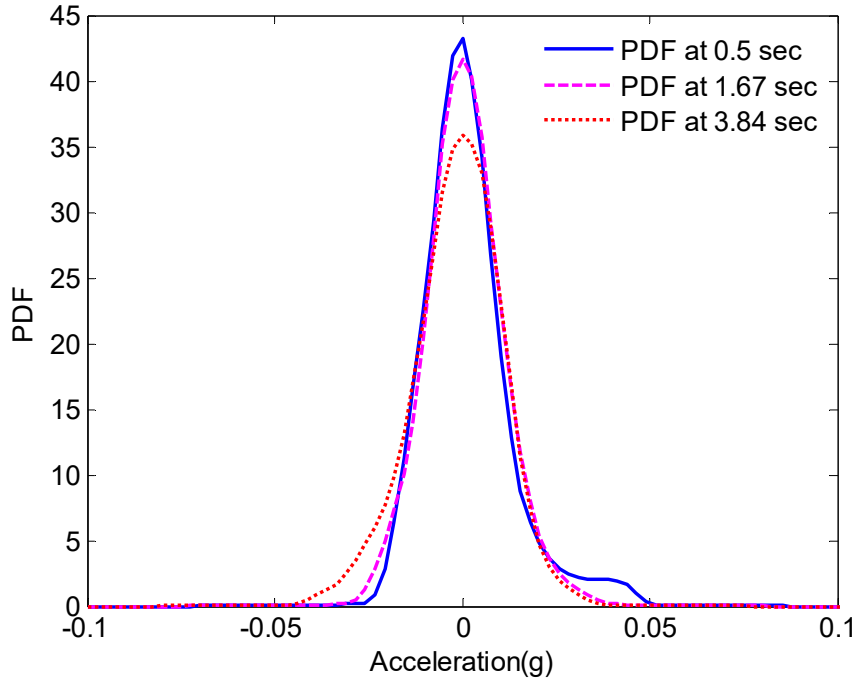

Figure 5. PDF of the acceleration response of the superstructure.

In Equation (28), $Y_q(\boldsymbol{\Theta}, t)(q = 1, 2, \cdots, N_{sel})$ is the acceleration dynamic time-history response of the superstructure. Therefore, the reliability defined in Equation (27) can be written as

$$\Pr = P\left\{\cup_{q=1}^{N_{sel}}(g_q(\boldsymbol{\Theta}, t) > 0)\right\} = P\{Z_{\max,T} > 0\} = \int_0^{\infty} p_{Z_{\max,T}}(z)\mathrm{d}z, \tag{29}$$

In Equation (29), $p_{Z_{\max,T}}$ is the PDF of $Z_{\max,\,T}$. Here, the PDF of the maximum values $Z_{\max,T}$ of the set of all dynamic time-history response of superstructure can be obtained by numerically solving the aforementioned density evolution Equation (26). From Equation (28), $Z_{\max,T}$ is obviously dependent on $\boldsymbol{\Theta}$; that is, $Z_{\max,T}$ is a function of $\boldsymbol{\Theta}$. Therefore, the form of $Z_{\max,T}$ with respect to $\boldsymbol{\Theta}$ can be obtained:

$$Z_{\max,T} = V(\boldsymbol{\Theta}, T), \tag{30}$$

Then, a virtual stochastic process with τ as virtual time may be constructed:

$$Z(\tau) = \varphi(V(\boldsymbol{\Theta}, T), \tau) = \phi(\boldsymbol{\Theta}, \tau). \tag{31}$$

The value of the stochastic process at a given time instant τ_c is equal to the extreme value in Equation (30):

$$Z(\tau_c) = \varphi(V(\boldsymbol{\Theta}, T), \tau_c) = \phi(\boldsymbol{\Theta}, \tau_c) = V(\boldsymbol{\Theta}, T). \tag{32}$$

In doing this, the velocity $\dot{\phi}(\theta, \tau) = \frac{\partial\phi(\theta,\tau)}{\partial\tau}$ may be substituted into Equations (25) and (26), and the PDF $p_{Z_{\max,T}}(z) = p_Z(z, \tau)|_{\tau=\tau_c} = p_Z(z, \tau_c)$ of equivalent extreme value $Z_{\max,T}$ may be obtained based on the finite difference numerical method.

By constructing the equivalent extreme events [34] of several acceleration responses of the superstructure, the extreme PDF (Figure 6) and the cumulative distribution function (Figure 7) of the vibration acceleration response of a superstructure can be obtained.

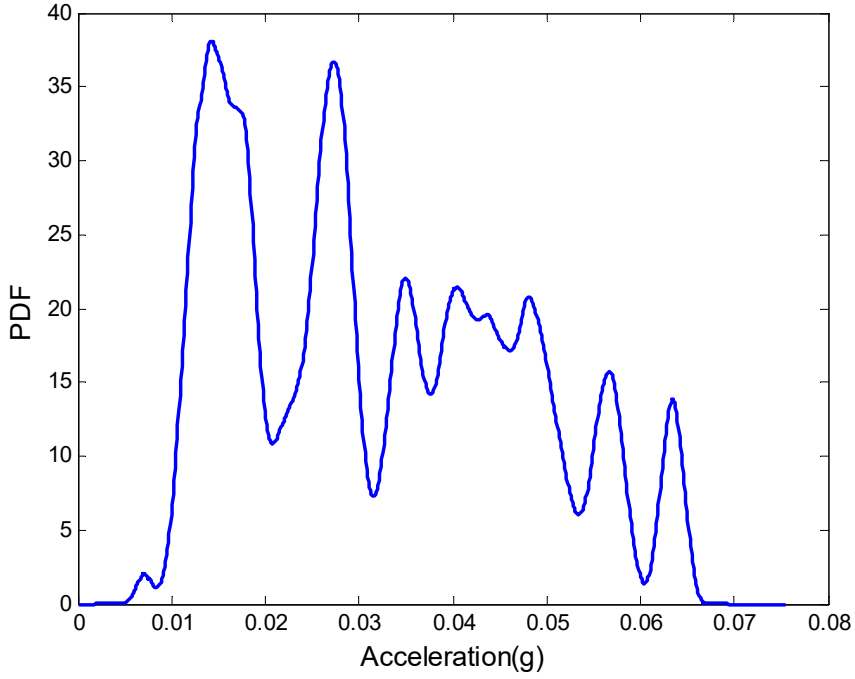

Figure 6. PDF of an equivalent extreme value event of floor acceleration.

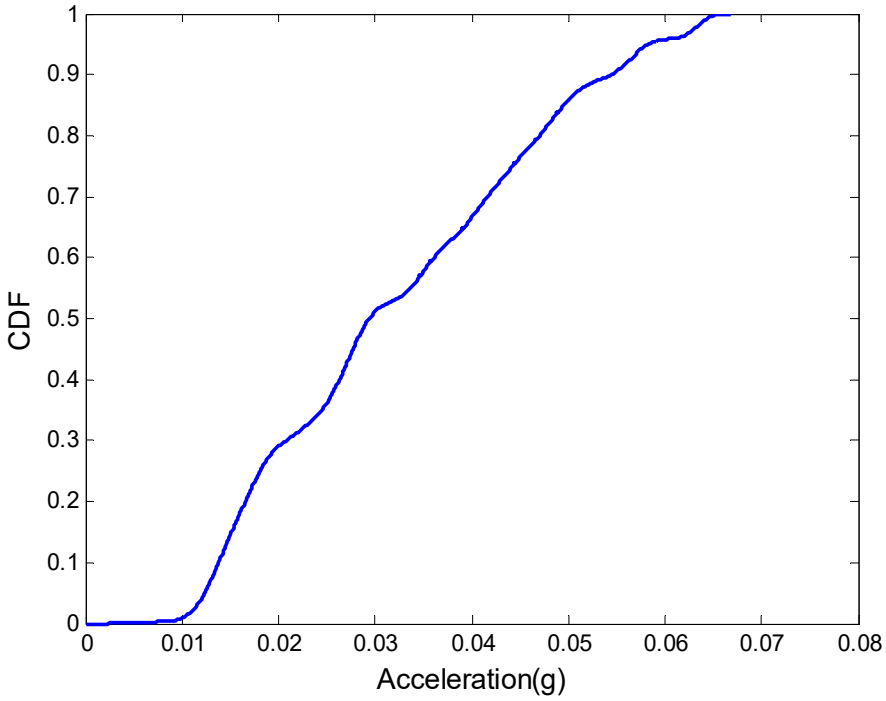

Figure 7. Vibration comfort reliability of the superstructure represented by acceleration.

The comfort levels of the tunnel superstructure under the impact of subway-vibration excitation can be characterized through the vibration-acceleration response of the building. According to different national design codes [39–41], various acceleration thresholds can be selected to evaluate the comfort reliability of building vibrations. The specific reliabilities are presented in Table 2. Under the control of the industrial vibration comfort standard, the reliability of the vibration comfort levels of the building satisfies the specifications (Table 2); that is, the vibration comfort dynamic reliability is $R_{\text{ind}} = 1$. However, under the control of the residential comfort acceleration standard, the vibration comfort reliability of the building is $R_{\text{res}} = 0.8763$, which is not perfect, indicating that the comfort requirements of the building under the action of some subway-vibration impact forces do not meet the specifications. Moreover, some isolation measures may be taken to achieve a vibration comfort of the building that meets the specifications at the dynamic reliability level.

Table 2. Vibration comfort level reliability of the tunnel superstructure.

Threshold Value	Reliability	Threshold Category
0.05 g	$R_{\text{res}} = 0.8763$	Vibration comfort requirements of residential buildings
0.08 g	$R_{\text{ind}} = 1$	Vibration comfort requirements for industrial plants

Note: "res" indicates the residential building and "ind" represents the industrial plant.

4. Long-Term Settlement Performance Evaluation of Soft Soil Foundation under Subway-Traffic Loads

Under subway-vibration excitation, with operation-time extension, the settlement of the tunnel soil shows a long-term effect. This type of long-term settlement threatens the safe subway operation. This section evaluated the long-term performance of the subway-tunnel foundation under subway-vibration excitation by integrating the long-term settlement mathematical model and the first-passage reliability theory.

4.1. Mathematical Prediction Model of Long-Term Settlement

The long-term settlement of the subgrade soil under the train load is a function of dynamic deviatoric stress (σ_d), static deviatoric failure stress (σ_s), and cumulative plastic

strain (ε_p). The dynamic additional settlement (long-term settlement) of the foundation can be expressed as follows:

$$s(t) = \int_0^h \varepsilon_p \mathrm{d}h, \tag{33}$$

where $s(t)$ is the long-term settlement and h is the foundation depth. The cumulative plastic strain of the soil layer under the long-term subway-traffic load can be obtained using Equation (34):

$$\varepsilon_p = (a + c \ln \omega) \left(\frac{\sigma_d}{\sigma_s} \right)^m n^b, \tag{34}$$

where n is the number of cyclic loading and is related to the number of metro train sections, departure times, and running times. a, c, m, and b are the fitting parameters. The frequency ω and the dynamic deflection stress σ_d are determined using the numerical results of the nonlinear dynamic finite element analysis.

The validity of the aforementioned mathematical model for the long-term settlement of the tunnel soil under subway-vibration excitation is verified by comparing the results between the numerical calculation and the experimental analyses (Figure 8) [42].

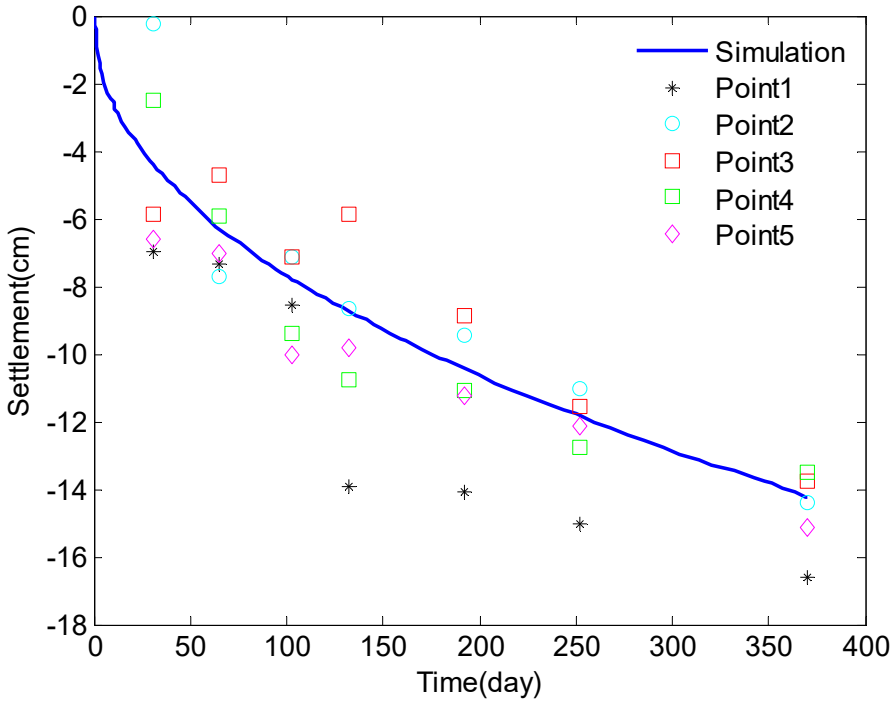

Figure 8. Validation of the long-term settlement model by using the simulation result and measured data (source data: [42]).

Figure 8 shows the comparison between the settlement data of the soft soil foundation measured at the first, second, third, fourth, and fifth measuring points in the throat area of the metro depot and the settlement values calculated using the proposed cumulative plastic strain model. In Figure 8, the scattered points are the settlement monitoring data, and the curve is the settlement of numerical simulation through nonlinear FEM. Figure 8 shows that the cumulative settlement calculated using the long-term settlement mathematical model is in strong agreement with the measured data, and the model can be used in the evaluation of the probabilistic performance of the tunnel foundation.

From the verification of the mathematical model, the proposed model can be used to accurately calculate the cumulative plastic strain of the foundation soil under the subway-train load at any number of cycles and predict the cumulative settlement of the foundation at any time.

4.2. Long-Term Settlement Prediction and Time-Dependent Reliability

Under the action of subway-vibration excitation, randomness is transferred from load excitation to a time-varying dynamic response through the superstructure–tunnel-soil physical dynamic system. The randomness of load excitation can be represented by the stochastic dynamic model of subway-vibration excitation, and the time histories of the vibration-excitation samples with rich probability characteristics of the same set system can be generated.

Furthermore, several long-term settlement time histories of the subway tunnel foundation can be obtained by combining the nonlinear finite-element dynamic analyses and the mathematical model of long-term settlement prediction. Thus, combined with PDET, the long-term settlement performance of the tunnel foundation can be evaluated from the perspective of time-varying reliability.

The long-term settlement $\boldsymbol{S} = \{S_q\}(q = 1, 2, \cdots N_{sel},)$ of the subway tunnel foundation can be obtained by substituting several dynamic deviatoric stresses $\sigma_{d,q}(q = 1, 2, \cdots, N_{sel})$ of the same set calculated in the nonlinear finite-element analysis into Equations (33) and (34). Furthermore, by substituting the settlement-time history $\dot{S}_q = \left\{\dot{S}_1, \dot{S}_2, \cdots, \dot{S}_{N_{sel}}\right\}$ as the velocity into the density-evolution equation, Equation (24), the PDEE of the tunnel foundation settlement can be acquired.

$$\frac{\partial p_{\boldsymbol{S\Theta}}(\boldsymbol{s}, \boldsymbol{\theta}, t)}{\partial t} + \dot{\boldsymbol{S}}(\boldsymbol{\theta}, t)\frac{\partial p_{\boldsymbol{S\Theta}}(\boldsymbol{s}, \boldsymbol{\theta}, t)}{\partial s} = -\mathcal{H}[S(s, \boldsymbol{\theta}, t)]p_{\boldsymbol{S\Theta}}(\boldsymbol{s}, \boldsymbol{\theta}, t). \tag{35}$$

In Equation (35), $\mathcal{H}[S(s, \boldsymbol{\theta}, t)]$ is the Heaviside indicator function, and its mathematical expression for tunnel foundation settlement can be written as

$$\mathcal{H}[S(s, \theta, t)] = \begin{cases} 0, S(s, \theta, t) < S_0 \\ 1, (s, \theta, t) \geq S_0 \end{cases}. \tag{36}$$

Here, S_0 is the subway vibration settlement threshold of the tunnel foundation, and the foundation settlement $S(s, \theta, t)$ of the tunnel due to vibration is less than and greater than or equal to threshold value S_0, corresponding to the safety domain and failure domain of time-varying reliability analysis, respectively. In addition, it should be noted that the above indicator function corresponds to the probability absorption boundary of general time-varying reliability analysis; that is, the PDF corresponding to the tunnel foundation settlement-time process when the settlement exceeds the threshold value S_0 is absorbed by the absorption boundary, but the probability information in the security domain will remain.

By solving Equation (35) combined with the first-passage theory [33,34], the abundant probability information of the long-term settlement of the tunnel foundation and time-dependent reliability $R(t)$ under different thresholds can be acquired.

$$R(t) = \int_{\Omega}\int p_{\boldsymbol{S\Theta}}(\boldsymbol{s}, \boldsymbol{\theta}, t)\mathrm{d}\boldsymbol{\theta}\mathrm{d}\boldsymbol{s}. \tag{37}$$

According to the definition of reliability, in Equation (37), Ω is the safety region. Combined with the first-passage theory and the PDFs of the dynamic response of the superstructure–tunnel system, after the dynamic deformation settlement response $s(t)$ enters the failure region, the PDF carried by it is absorbed and does not return to the safety region. Therefore, the integral of the PDF on the safety region is reliability $R(t)$. Obviously, the key to the time-varying reliability calculation here is to obtain the PDF of tunnel foundation settlement evolution with time under the threshold absorption boundary.

The statistical characteristics (mean value $E(X)$ and the standard deviation $\sqrt{D(x)}$) of the long-term settlement of the tunnel foundation with time evolution are shown in Figure 9; they are the same as the previous vibration comfort assessment of the superstructure characterized by acceleration. At the same time, Figure 9 further verifies the rationality

of the time-varying reliability analysis of tunnel-foundation vibration settlement in this study from the side. This is because, in this study, the rationality of the mean and variance calculation is affected by the PDF (p); that is:

$$\begin{cases} E(X) = \int_{\Omega} x \cdot p \mathrm{d}x \\ D(x) = \int_{\Omega} [x - E(x)]^2 \cdot p \mathrm{d}x \end{cases} \tag{38}$$

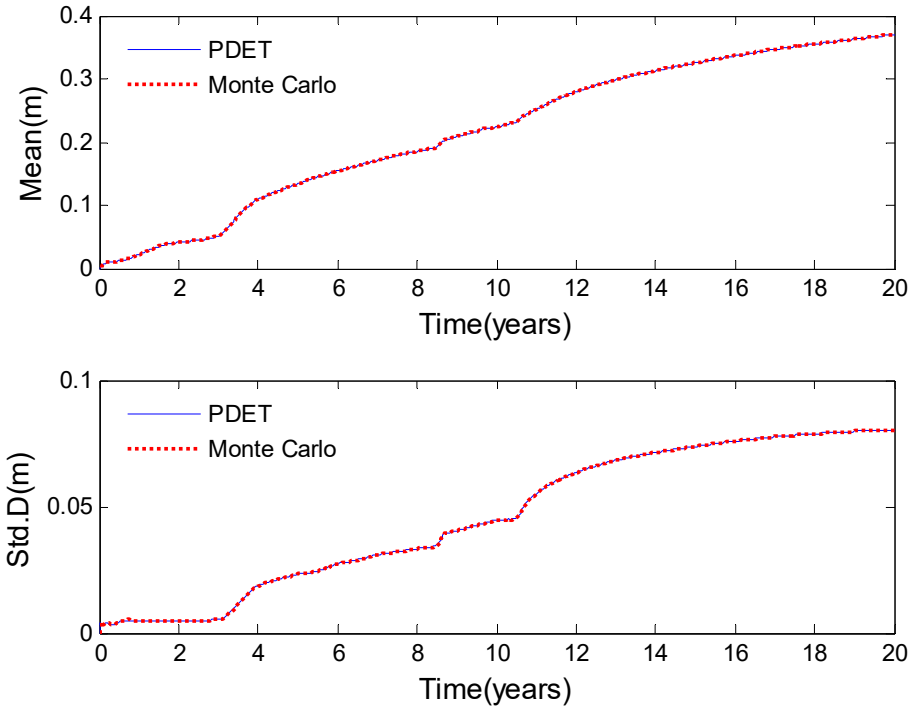

Figure 9. Evolution of the mean and standard deviations of the long-term settlement of the subway track with time.

Obtaining a higher precision numerical solution of the PDF is an important prerequisite for obtaining the mean and variance. Therefore, the statistics of the long-term settlement of the tunnel foundation caused by operation vibration (Figure 9) also indirectly prove the rationality and effectiveness of this study.

Figure 10 shows the reliability distribution of the long-term settlement deformation of a subway track under different threshold indicators. The reliability evolution mechanism of subway track foundation vibration deformation is not the same under different thresholds (Figure 10). However, the vibration reliability of the subway completely satisfies the design requirements for almost five years before the subway comes into operation. With time, due to the influence of subway-operation vibration, its reliability begins to decay. For different safe-operation deformation-control thresholds, various reinforcement maintenance time points can be determined using reliability evolution. This study can provide a data reference for making decisions regarding the healthy operation of subway tracks. The specific dynamic reliability of subway tunnels with different thresholds and service years under vibration impact is presented in Table 3. When the requirements for vibration settlement control are high, for example, if the control standard threshold is 0.15 m, the service life or maintenance time may be 15 years.

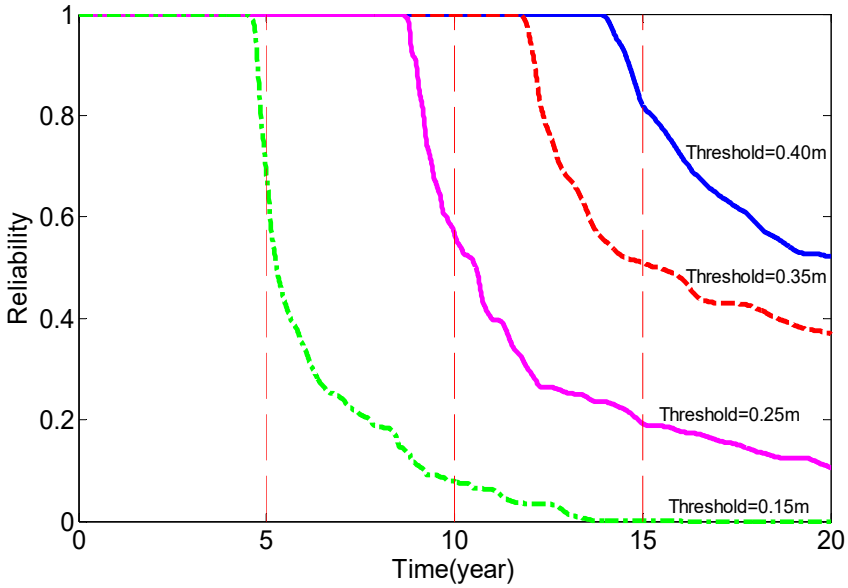

Figure 10. Time-dependent reliability of the long-term settlement deformation of the subway track.

Table 3. Time-dependent reliability of the long-term settlement deformation of the subway track.

Service Life (Years)	Threshold Value (m)	Reliability
5	0.15	0.6513
	0.25	1.0
	0.35	1.0
	0.40	1.0
10	0.15	0.0642
	0.25	0.5826
	0.35	1.0
	0.40	1.0
15	0.15	0
	0.25	0.1987
	0.35	0.5734
	0.40	0.8112
20	0.15	0
	0.25	0.1125
	0.35	0.3756
	0.40	0.5224

5. Conclusions

By conducting comprehensive analyses for evaluating the performance of a superstructure--tunnel soil system under subway-vibration excitation and considering the randomness of subway-vibration excitation, the time-varying performance of the superstructure and the subway tunnel foundation was evaluated from the perspective of probabilistic performance evolution. The specific conclusions are as follows:

(1) Considering the random track irregularity and the constant train axle load, the power spectrum of the train-excitation-impact force was obtained based on the PEM. Furthermore, based on the spectrum representation and the random function idea, the sample time histories and corresponding probability of the random excitation load of the same set of trains were established.

(2) According to nonlinear dynamic finite-element time-history analysis and the long-term settlement mathematical prediction model, the dynamic responses of the superstructure and tunnel foundation were studied. Based on the dynamic reliability of the vibration acceleration of the superstructure, its comfort under the impact of subway vibration was

evaluated. This study provided a new reliability index method for the vibration-impact assessment of the subway superstructure, which evaluated the vibration dynamic-safety performance of the superstructure from two different perspectives: residential comfort and industrial vibration-control requirements.

(3) Based on PDET and first-passage theory, the long-term performance of the superstructure and the tunnel foundation was evaluated from the perspectives of PDF and probabilistic performance evolution. For the subway tunnel foundation with a high-control standard of foundation vibration settlement, its service life or maintenance and its reinforcement time was predicted from the perspective of time-varying reliability.

Author Contributions: Conceptualization, L.W. and S.Y.; methodology, H.H.; validation, L.W.; formal analysis, H.H.; writing—original draft preparation, L.W. and H.H.; writing—review and editing, L.W., S.Y. and H.H.; visualization, L.W. All authors have read and agreed to the published version of the manuscript.

Funding: This research was funded by National Natural Science Foundation of China, grant number 42002272, and the fellowship of China Postdoctoral Science Foundation, grant number 2021M702791.

Data Availability Statement: Not applicable.

Conflicts of Interest: The authors declare no conflict of interest.

References

1. Kurzweil, L.G. Ground-borne noise and vibration from underground rail systems. *J. Sound Vib.* **1979**, *66*, 363–370. [CrossRef]
2. Yang, Y.B.; Hung, H.H. Soil Vibrations Caused by Underground Moving Trains. *J. Geotech. Geoenvironmental Eng.* **2008**, *134*, 1633–1644. [CrossRef]
3. Liang, X.; Yang, Y.B.; Ge, P.; Hung, H.H.; Wu, Y. On computation of soil vibrations due to moving train loads by 2.5d approach. *Soil Dyn. Earthq. Eng.* **2017**, *101*, 204–208. [CrossRef]
4. Yuan, Z.; Cao, Z.; Tang, H.; Xu, Y.; Wu, T. Analytical layer element with a circular cavity and its application in predicting ground vibrations from surface and underground moving sources. *Comput. Geotech.* **2021**, *137*, 104262. [CrossRef]
5. Yuan, Z.; Bostrom, A.; Cai, Y.; Cao, Z. Analytical solution for calculating vibrations from twin circular tunnels. *Soil Dyn. Earthq. Eng.* **2019**, *117*, 312–327. [CrossRef]
6. Qu, S.; Yang, J.; Feng, Y.; Peng, Y.; Zhao, C.; Zhu, S.; Zhai, W. Ground vibration induced by maglev trains running inside tunnel: Numerical modelling and experimental validation. *Soil Dyn. Earthq. Eng.* **2022**, *157*, 107278. [CrossRef]
7. Zhu, C.; Cheng, H.; Bao, Y.; Chen, Z.; Huang, Y. Shaking table tests on the seismic response of slopes to near-fault ground motion. *Geomech. Eng* **2022**, *29*, 133–143.
8. Mao, W.; Xu, C.; Yang, Y. Investigation on strength degradation of sandy soil subjected to concentrated particle erosion. *Environ. Earth Sci.* **2022**, *81*, 1–10. [CrossRef]
9. Scislo, L.; Guinchard, M. Source based measurements and monitoring of ground motion conditions during civil engineering works for high luminosity upgrade of the LHC. In Proceedings of the 26th International Congress on Sound and Vibration, Montreal, QC, Canada, 7–11 July 2019.
10. Lacny, L.; Scislo, L.; Guinchard, M. Application of probabilistic power spectral density technique to monitoring the long-term vibrational behaviour of CERN seismic network stations. *Vib. Phys. Syst.* **2020**, *31*, 2020311.
11. Fiala, P.; Degrande, G.; Augusztinovicz, F. Numerical modelling of ground-borne noise and vibration in buildings due to surface rail traffic. *J. Sound Vib.* **2007**, *301*, 718–738. [CrossRef]
12. Chai, J.C.; Miura, N. Traffic-load-induced permanent deformation of road on soft subsoil. *J. Geotech. Geoenvironmental Eng.* **2002**, *128*, 907–991. [CrossRef]
13. Li, D.; Selig, E.T. Cumulative plastic deformation for fine-grained subgrade soils. *J. Geotech. Eng.* **1996**, *122*, 1006–1013. [CrossRef]
14. Monismith, C.L.; Ogawa, N.; Freeme, C.R. Permanent deformation characteristics of subgrade soils due to repeated loading. *Transp. Res. Rec.* **1975**, *537*, 1–17.
15. Beskou, N.D.; Theodorakopoulos, D.D. Dynamic effects of moving loads on road pavements: A review. *Soil Dyn. Earthq. Eng.* **2011**, *31*, 547–567. [CrossRef]
16. Kumar, P.; Chattopadhyay, A.; Mahanty, M.; Singh, A.K. Stresses induced by a moving load in a composite structure with an incompressible poroviscoelastic layer. *J. Eng. Mech.* **2019**, *145*, 04019062. [CrossRef]
17. Mahanty, M.; Chattopadhyay, A.; Kumar, P.; Singh, A.K. Effect of initial stress, heterogeneity and anisotropy on the propagation of seismic surface waves. *Mech. Adv. Mater. Struct.* **2020**, *27*, 177–188. [CrossRef]
18. Mahanty, M.; Kumar, P.; Singh, A.K.; Chattopadhyay, A. Dynamic response of an irregular heterogeneous anisotropic poroelastic composite structure due to normal moving load. *Acta Mech.* **2020**, *231*, 2303–2321. [CrossRef]
19. Shi, W.; Bai, L.; Han, J. Subway-induced vibration measurement and evaluation of the structure on a construction site at curved section of metro line. *Shock. Vib.* **2018**, *2018*, 1–18. [CrossRef]

20. Xin, L.; Li, X.; Zhu, Y.; Liu, M. Uncertainty and sensitivity analysis for train-ballasted track–bridge system. *Veh. Syst. Dyn.* **2019**, *58*, 1–19. [CrossRef]
21. Bortolini, R.; Forcada, N. A probabilistic-based approach to support the comfort performance assessment of existing buildings. *J. Clean. Prod.* **2019**, *237*, 117720. [CrossRef]
22. Kim, Y.; Han, J.; Chun, C. Evaluation of comfort in subway stations via electroencephalography measurements in field experiments. *Build. Environ.* **2020**, *183*, 107130. [CrossRef]
23. Mao, J.F.; Xiao, Y.J.; Yu, Z.W.; Tutumluer, E.; Zhu, Z.H. Probabilistic model and analysis of coupled train-ballasted track-subgrade system with uncertain structural parameters. *J. Cent. South Univ.* **2021**, *28*, 2238–2256. [CrossRef]
24. Zhu, C.; Huang, Y.; Sun, J. Solid-like and liquid-like granular flows on inclined surfaces under vibration–Implications for earthquake-induced landslides. *Comput. Geotech.* **2020**, *123*, 103598. [CrossRef]
25. Mao, W.; Hamaguchi, H.; Koseki, J. Discrimination of particle breakage below pile tip after model pile penetration in sand using image analysis. *Int. J. Geomech.* **2020**, *20*, 04019142. [CrossRef]
26. Lombaert, G.; Degrande, G. Ground-borne vibration due to static and dynamic axle loads of intercity and high-speed trains. *J. Sound Vib.* **2009**, *319*, 1036–1066. [CrossRef]
27. Sheng, X.; Jones, C.J.C.; Thompson, D.J. A theoretical model for ground vibration from trains generated by vertical track irregularities. *J. Sound Vib.* **2004**, *272*, 937–965. [CrossRef]
28. Lin, J.H.; Zhang, Y.H. *Pseudo-Excitation Method for Random Vibration*; Science Press: Beijing, China, 2004.
29. Scislo, L.; Lacny, L.; Guinchard, M. COVID-19 lockdown impact on CERN seismic station ambient noise levels. *Open Eng.* **2021**, *11*, 1233–1240. [CrossRef]
30. Lei, X.Y. *High Speed Railway Track Dynamics: Models, Algorithms and Applications*; Science Press and Springer Nature: Beijing, China, 2017.
31. Chen, G.; Zhai, W.M.; Zuo, H.F. Analysis of the random vibration responses characteristics of vehicle-track coupling system. *J. Traffic Transp. Eng.* **2001**, *1*, 13–16.
32. Li, J.; Chen, J.B. The principle of preservation of probability and the generalized density evolution equation. *Struct. Saf.* **2008**, *30*, 65–77. [CrossRef]
33. Li, J. A PDEM-based perspective to engineering reliability: From structures to lifeline networks. *Front. Struct. Civ. Eng.* **2020**, *14*, 1056–1065. [CrossRef]
34. MIDAS GEOTECH, 2D & 3D Geotechnical Finite Element Analysis. 2022. Available online: https://www.midasgeotech.com/solution/gtsnx (accessed on 22 February 2023).
35. Schanz, T.; Vermeer, P.A.; Bonnier, P.G. *The Hardening Soil Model: Formulation and Verification*; Beyond 2000 in Computation Geotechnics-10 Years of PLAXIS; Routledge: Oxfordshire, UK, 1999; pp. 281–296. ISBN 90 5809 040X.
36. Hu, H.; Huang, Y.; Zhao, L.; Xiong, M. Shaking table tests on slope reinforced by anchored piles under random earthquake ground motions. *Acta Geotech.* **2022**, *17*, 4113–4130. [CrossRef]
37. Hu, H.; Gan, G.; Bao, Y.; Guo, X.; Xiong, M.; Han, X.; Wang, L. Nonlinear Stochastic Seismic Response Analysis of Three-Dimensional Reinforced Concrete Piles. *Buildings* **2023**, *13*, 89. [CrossRef]
38. Hu, H.; Huang, Y.; Xiong, M.; Zhao, L. Investigation of seismic behavior of slope reinforced by anchored pile structures using shaking table tests. *Soil Dyn. Earthq. Eng.* **2021**, *150*, 106900. [CrossRef]
39. Standard for Allowable of Building Engineering. *GB 50868-2013*; China Planning Press: Beijing, China, 2013.
40. *DIN 4150-3*; Structural Vibration. Part 3: Effects of Vibration on Structures. 1999. Available online: https://webstore.ansi.org/standards/din/din41502016 (accessed on 22 February 2023).
41. *BS 7385-2*; Evaluation and Measurement for Vibration in Buildings. Part 2: Guide to Damage Levels from Ground Borne Vibration. 1993. Available online: https://www.en-standard.eu/bs-7385-2-1993-evaluation-and-measurement-for-vibration-in-buildings-guide-to-damage-levels-from-groundborne-vibration/ (accessed on 22 February 2023).
42. Chen, Y.K.; Wang, Y.M.; Zou, C.; Zhou, J.P.; Kuang, Y.Q.; Xu, J.H. *Long-Term Settlement Analysis and Settlement Control Technology of Rheological Soft Soil Caused by Metro Train Vibration*; Research Report; Guangzhou Metro Group Co. Ltd.: Guangzhou, China, 2017.